Article

Optimization and Characterization of a Novel Antioxidant Naringenin-Loaded Hydrogel for Encouraging Re-Epithelization in Chronic Diabetic Wounds: A Preclinical Study

Neha Raina, Shafiul Haque, Hardeep Singh Tuli, Atul Jain, Petr Slama, and Madhu Gupta*

Cite This: *ACS Omega* 2023, 8, 34995−35011

Read Online

ACCESS | Metrics & More | Article Recommendations

ABSTRACT: Nonhealed wounds are one of the most dangerous side effects of type-2 diabetes, which is linked to a high frequency of bacterial infections around the globe that eventually results in amputation of limbs. The present investigation aimed to explore the drug-loaded (naringenin) hydrogel system for chronic wound healing. The hydrogel membranes comprising Na-alginate with F-127 and poly(vinyl alcohol) were developed to treat chronic wounds using the quality-by-design (QbD) approach. The optimized formulation was tested for various parameters, such as swelling, gel fraction, water vapor transition rate (WVTR), etc. *In vitro* evaluation indicated that a drug-loaded hydrogel displayed better tissue adhesiveness and can release drugs for a prolonged duration of 12 h. Scratch assay performed on L929 cell lines demonstrated good cell migration. The diabetic wound healing potential of the hydrogel membrane was assessed in streptozotocin-induced male Wistar rats (50 mg/kg). Higher rates of wound closure, re-epithelialization, and accumulation of collagen were seen in *in vivo* experiments. Histopathologic investigation correspondingly implied that the drug-loaded hydrogel could enhance dermal wound repair. The improved antimicrobial and antioxidant properties with expedited healing indicated that the drug-loaded hydrogel is a perfect dressing for chronic wounds.
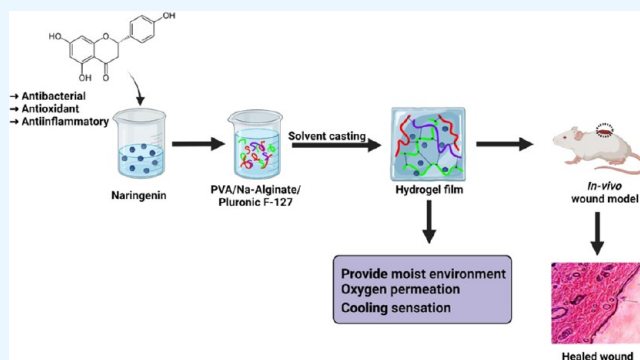
INTRODUCTION

Diabetes mellitus is a frequently diagnosed chronic condition that has already adversely affected many individuals around the globe. Its prevalence is expected to rise to 439 million new cases by 2030.[1] Wounds in individuals who have diabetes do not heal in the usual prompt, effective, and structured way; rather, they tend to remain in a chronic phase of the disease. Furthermore, diabetes impairs the processes of neutrophils and macrophages, restricts the migratory potential of keratinocytes and fibroblasts, minimizes growth factor responses, and tends to increase apoptosis.[2] Healing is a dynamic process that is divided into four progressive, extreme, and systematic stages, namely, hemostasis, inflammation, proliferation, and remodeling.[3] The events of each phase must take place in a controlled manner. Dehydration of wounds and infection leads to incurable wounds, and therefore, keeping the wound bed moist is very important for healing the wound effectively.[4] Hydrogel is considered a potential dressing as it can retain more water in its network and absorb the wound exudate; bioactive compounds can be loaded effectively in the hydrogel system, providing delivery of drugs in a controlled manner.[5] The hydrogel fabricated using biopolymers will be beneficial and efficient in treating diabetic wounds, as biopolymers have their healing action.[6,7]

Alginate is an anionic biopolymer found in brown algae, composed of monosaccharide units of 1,4-linked-l-guluronic acid residue and 1,4-linked-D-mannuronic acid residue.[8] Alginate has therapeutic properties and can be used to heal both acute and chronic wounds. Alginate is absorbent in nature and can be used to treat medical issues, such as burns. Alginates have an excellent affinity for pathogenic microbes, which aids in wound infection prevention and minimizes the need for dressings.[9] When in contact with wound exudates, alginates partly dissolve and form a hydrophilic gel that maintains a moisturizing effect on the wound.[10] Also, it helps boost cell proliferation and tissue granulation, which leads to a faster healing process. Alginates have limited therapeutic relevance despite their optimal wound healing capabilities

due to their mechanical performance and low tensile features. As a result, alginate is often coupled with some other polymer parts to enhance its controllability and increase cell adherence and stability.[11]

Therefore, a hydrogel-containing Na-alginate with thermo-sensitive polymer (F-127) and poly(vinyl alcohol) (PVA), an active film former, was designed for chronic wounds. The hydrogels fabricated by using PVA are widely used as biomaterials in the treatment of wounds. It is the most widely used synthetic polymer in wound care, contact lenses, and drug delivery devices. It is successfully used to treat chronic wounds due to its fundamental hydrophilicity, massive water permeability, and large swelling capacity.[12] However, several drawbacks, such as insufficient elasticity and the creation of a stiff membrane, limit its use as a hydrogel membrane. F-127 is a nonionic surfactant reported to be nontoxic and beneficial in topical and ophthalmic preparations without skin irritation or sensitivity. The composite hydrogels fabricated using polymers of synthetic origin are reported to perform well as drug carriers; therefore, adding F-127 can increase hydrophobic drug solubility; this surfactant is also used in formulations for wound healing.[13] As chronic wounds gets stuck in the inflammatory phase, bacterial invasion is the common problem faced by chronic wounds; so, the addition of efficient therapeutic agents with antioxidant, anti-inflammatory, and antimicrobial properties would be beneficial for expedited wound healing.[14,15]

Therefore, naringenin (4,5,7-trihydroxy flavanone) (Nar) is a flavonoid capable of eradicating superoxide and hydroxyl radicals and shows antibacterial activity against different species of bacteria. It has strong potential in scavenging the free radicals and reducing oxidative DNA damage caused by lipid peroxidation, which could be used to treat inflammatory disorders.[16] So, naringenin was incorporated into the hydrogel system. Furthermore, these novel hydrogel membranes will enable sustained release superficially at the wound site, enhancing the drug concentration at the site. A scientifically validated, systematic risk-based method called "quality-by-design" (QbD) aids in interpreting and managing the relationship between critical process parameters (CPPs) and critical quality attributes (CQAs), both of which are important for the development of high quality target product profiles (QTPPs) carried out on this formulation.[17,18] Critical material parameters (CMPs) and critical process parameters (CPPs), such as mechanical strength and swelling, or essential attributes of quality (CQAs), such as desired concentrations of respective polymers for gel formation, were chosen. Box−Behnken design (BBD) is employed for the optimization process. Swelling and mechanical strength were chosen as the design's response variables. As a result, the systematic production of a drug-loaded hydrogel for chronic wounds using QbD principles is the focus of the study in the current investigation.

■ RESULTS AND DISCUSSION

Optimization Studies. A second-order quadratic polynomial model was fitted to the investigational data using Box−Behnken design, and the results showed significant correlation coefficient values and a significant "lack of model fitness." The coefficient evaluations of the polynomial models revealed important CQAs between the analyzed input factors and output variables. The matrix of 17 experimental runs for drug-loaded hydrogel at various levels of each assigned factor is summarized in Table 1 for reference, and the formulations

Table 1. Box−Behnken Design Enabled the Design Matrix for the Optimization of Drug-Loaded Hydrogel

run(s)	coded factor level		
	factor 1	factor 2	factor 3
1	0	0	0
2	+1	+1	0
3	+1	0	+1
4	0	+1	+1
5	0	0	0
6	+1	0	−1
7	−1	0	+1
8	−1	+1	0
9	0	−1	+1
10	0	−1	−1
11	0	0	0
12	0	0	0
13	−1	0	−1
14	+1	−1	0
15	−1	−1.	0
16	0	+1	−1
17	0	0	0
	level of factor studies		
selected factors	low (−1)	inter-medi-ate (0)	high (+1)
Na-alginate	3	4.5	6
PVA	3	4.5	6
Pluronic F-127	3	4.5	6

were tested for mechanical strength and swelling as the CQAs of the product. eq 1 displays the direct effects of the chosen elements as well as their interactions.[19]

$$Y = \beta^0 + \beta^1 X_1 + \beta^2 X_2 + \beta^3 X_3 + \beta^4 X_1 X_2 + \beta^5 X_1 X_3$$
$$+ \beta^6 X_2 X_3 + \beta^7 X_1^2 + + \beta^8 X_2^2 + \beta^9 X_3^2 \quad (1)$$

where β^0, β^1, β^2, and β^3 reflect the intercept and factor coefficients, viz., X_1, X_2 and X_3, respectively, β^4, β^5, and β^6 represent the coefficients of interaction terms between X_1 and X_2, X_1 and X_3, and X_2 and X_3, respectively, and β^7, β^8, and β^9 are the corresponding coefficients of quadratic terms, X_1^2, X_2^2, and X_3^2.

Table 2 includes the coefficients, R^2 values, and statistical significance (p) levels of different quadratic model terms that were used in the analysis of specific CQAs. The development of a thorough scientific knowledge of the potential factor−response relationship(s) among the selected CMAs/CPPs and the related CQAs was made possible by response surface methodology (RSM) tools. The 3D response surface and related 2D contour plots for the influence of each chosen CMA are shown in Figures 1a−f and 2a−f, viz., Na-alginate, PVA, and pluronic F-127 on studied CQAs like mechanical strength and swelling (%) of the prepared hydrogel. Figures 1a,c,e and 2a,c,e illustrate the curvilinear 3D response surface plots representing the response surface plots for mechanical strength and swelling (%), while the corresponding 2D contour plots represent the analogous information,[20,21] as depicted in Figures 1b,d,f and 2b,d,f.

Mechanical Strength. Figure 1 illustrates the curvilinear 3D response surface plot, signifying the response surface for the mechanical strength between Na-alginate and pluronic F-127. By increasing the Na-alginate concentration, the hydrogel's mechanical strength decreases, while inverse observation

Table 2. Coefficients of Polynomial Equation of Different Studied Critical Quality Attributes as per the Second-Order-Modified Quadratic Model

coefficient codes	polynomial coefficients for selected CQAs	
	tensile strength	swelling index
β^0	7.28	306.80
β^1	−0.3900	37.42
β^2	0.9162	−2.51
β^3	1.90	−1.50
β^4	1.27	7.43
β^5	0.0100	−4.53
β^6	−0.4375	−9.62
β^7	0.5438	7.37
β^8	1.49	−8.48
β^9	1.04	−18.46
p-value	<0.0001	<0.0019
R^2	0.9437	0.8456

was observed with an increase in the concentration of pluronic F-127. Keeping the minimum concentration of Na-alginate constant and increasing the pluronic F-127 concentration, minimum mechanical strength was observed at the mid-level of pluronic F-127. While keeping the low level of pluronic F-127 constant and increasing the Na-alginate concentration, a gradual increase in mechanical strength was observed, and a maximum strength was observed at a high level of pluronic F-127. An analogous result was observed in the corresponding 2D plot, as depicted in Figure 1b.

Figure 1c shows the 3D response surface plot, indicating the response surface for the mechanical strength between Na-alginate and PVA. By increasing the Na-alginate concentration, the hydrogel's mechanical strength decreases up to mid-level, followed by a plateau at a higher concentration of Na-alginate. While increasing the PVA concentration, a gradual increase in mechanical strength was observed, followed by a high concentration of PVA. Keeping the minimum concentration of Na-alginate constant and increasing the PVA concentration, maximum mechanical strength was observed at a high level of PVA. While keeping a low level of PVA constant and increasing the Na-alginate concentration, minimum mechanical strength was observed at the mid-level of Na-alginate. A similar observation is in the corresponding 2D contour plot, as observed in Figure 1d.

Figure 1e shows the inverted tilted canopy-shaped 3D response surface plot, indicating the response surface for the mechanical strength between pluronic-127 and PVA. By increasing the concentration of pluronic F-127, a slight decrease followed by a gradual increase in mechanical strength was initially observed in the hydrogel from a low to a high level of pluronic F-127. As the PVA concentration increases, a gradual increase in mechanical strength is observed at high concentrations of PVA. Keeping the low level of pluronic F-127 constant and increasing the PVA, maximum mechanical strength was observed at a high level of PVA. While maintaining a low level of PVA constant and increasing the pluronic F-127 concentration, minimum mechanical strength was observed at the mid-level of pluronic F-127. A similar observation is observed in the corresponding 2D contour plot, as observed in Figure 1f.

Swelling %. By increasing the concentration of Na-alginate, the swelling (%) of the hydrogel gradually increases up to the high level of Na-alginate, while a negligible swelling

(%) was observed with an increase in the concentration of pluronic F-127. Keeping the minimum concentration of Na-alginate constant and increasing the pluronic F-127 concentration, a minimum swelling (%) was observed at a high level of pluronic F-127. While keeping pluronic F-127 constant at a low level and increasing the concentration of Na-alginate, a gradual increase in the swelling % was observed from a low to high level of alginate. A similar analogous observation was observed in the corresponding 2D plot, as observed in Figure 2b. Figure 2c illustrates the 3D response surface plot, signifying the response surface for the swelling (%) between Na-alginate and PVA, indicating an observation similar to that observed and depicted in Figure 2a. A similar observation was portrayed in the corresponding 2D contour plot, as shown in Figure 2d. Figure 2e shows the canopy flattened umbrella-shaped 3D response surface plot representing the response surface for the swelling (%) between pluronic F-127 and PVA. The maximum swelling (%) of the prepared hydrogel was obtained at the mid-level of both factors. Figure 2 indicates similar analogous results in the corresponding 2D contour plots.

Search for Optimum Formulation. By "trading-off" different CQAs, the best formulation was chosen in order to get the required results, i.e., mechanical strength (time taken to break the hydrogel membrane) and swelling (%) (to provide a humid environment). Following the aforementioned conditions, the optimized drug-loaded hydrogel was achieved via numerical and graphical optimization techniques to bring the values of the desirability function closer to one. Figure 3 portrays the overlay space with the composition of the optimum drug-loaded hydrogel demarcated in the plot, such as Na-alginate (4.9), pluronic F-127 (4.9), and PVA (4.9), attaining mechanical strength of approximately 8 MPa (7.7) and swelling % of approximately 315% well within the design space.

FTIR Analysis. FTIR analysis of naringenin, Na-alginate, PVA, F-127, and hydrogel-loaded with the drug is illustrated in Figure 4. The peaks of the naringenin spectra at cm^{-1} can be attributed to O−H stretching. The peaks displayed in the graph at 1505 cm^{-1} (C=O stretching vibrations) stretching and 1062 cm^{-1} (C−O stretching) peak at 3257 cm^{-1} corresponding to the O−H stretching. Na-alginate spectrum displayed the functional group at 2897 cm^{-1} and 3364 cm^{-1} due to the −CH group and −OH streching vibrations, respectively. The peaks in the spectrum of PVA at 3566 cm^{-1} arise out of the O−H stretching frequency representing the presence of hydroxyl groups. The broad band at 1531 cm^{-1} and the peak at 3188 cm^{-1} in PVA are caused by the stretching vibrations of the −CO group and the formation of primary N−H amide bonds. The F-127 graph depicts a broad peak at 2789 cm^{-1} as a result of stretching vibrations of the −CH group and peaks visible at 1697 cm^{-1} (O−H bending) and 1085 cm^{-1} (C−O−C stretching vibrations). FTIR graphs of the drug-loaded hydrogel were examined to verify the unbound drug present in its network. The functional groups located at 3251 and 1515 cm^{-1} indicated a similar area as mentioned in the naringenin spectra. The presence of new peaks and abundant functional groups indicated that the polymers utilized were effectively cross-linked physically.[22]

XRD Analysis. The material crystallinity is revealed by the XRD spectrum (Figure 5). When studying materials, it is imperative to get a thorough understanding of microstructure since it influences the physical and mechanical qualities of the product. Hence, the crystalline structure of blank hydrogel,
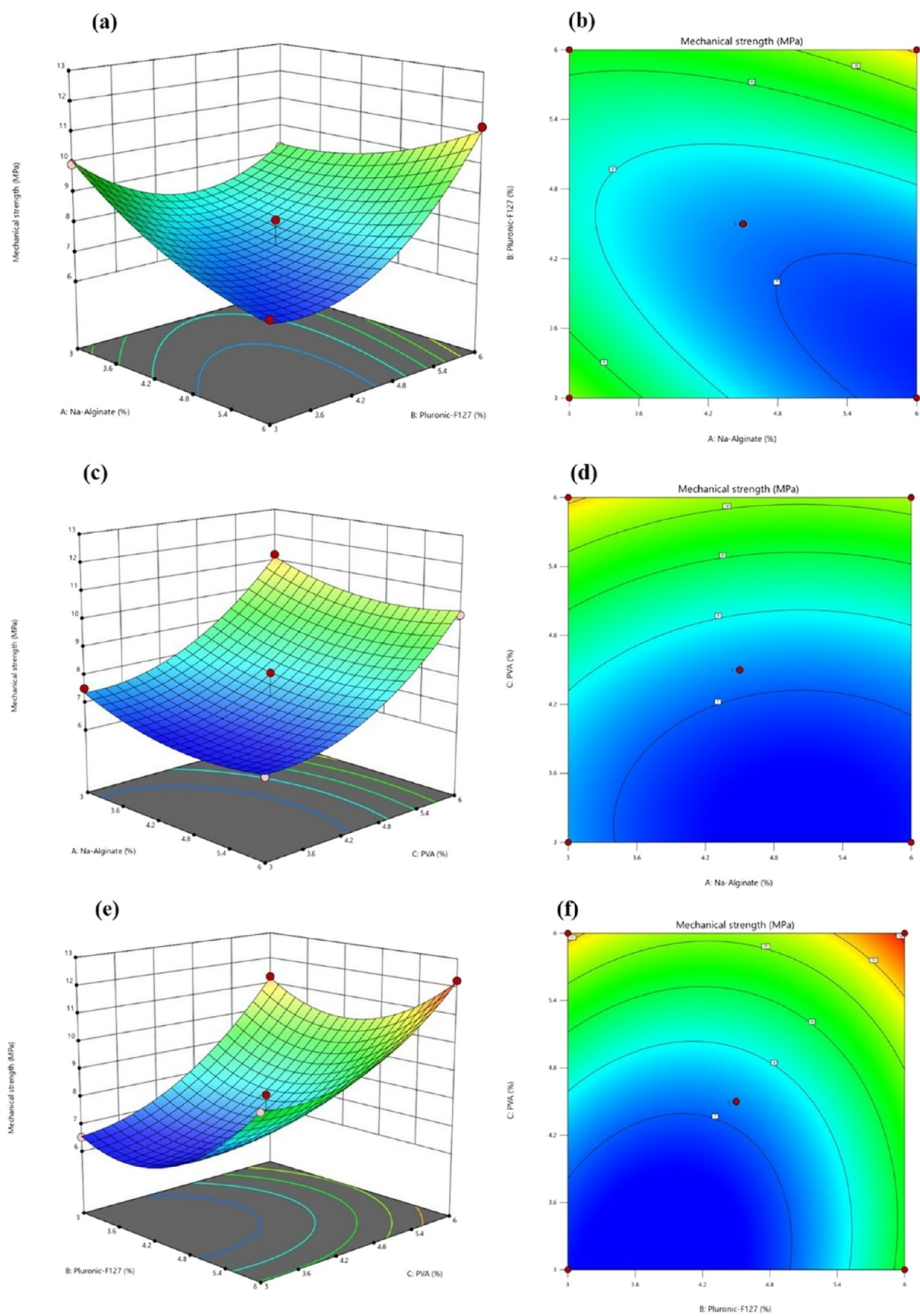
Figure 1. 3D response surface plots and 2D contour plots of mechanical strength with respect to the concentration of polymers.
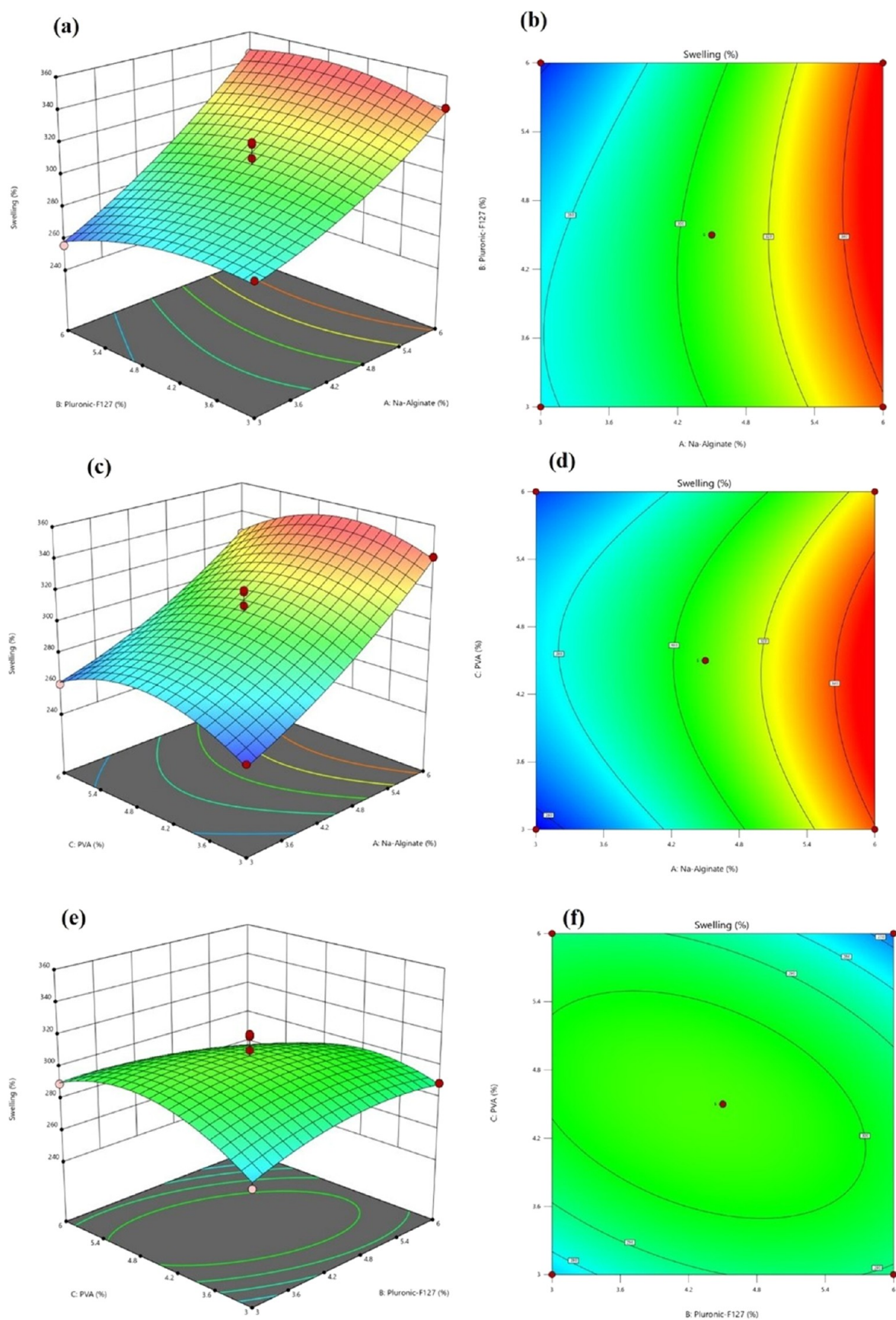
Figure 2. 3D response surface plots and 2D contour plots of swelling % with respect to the polymer concentration.
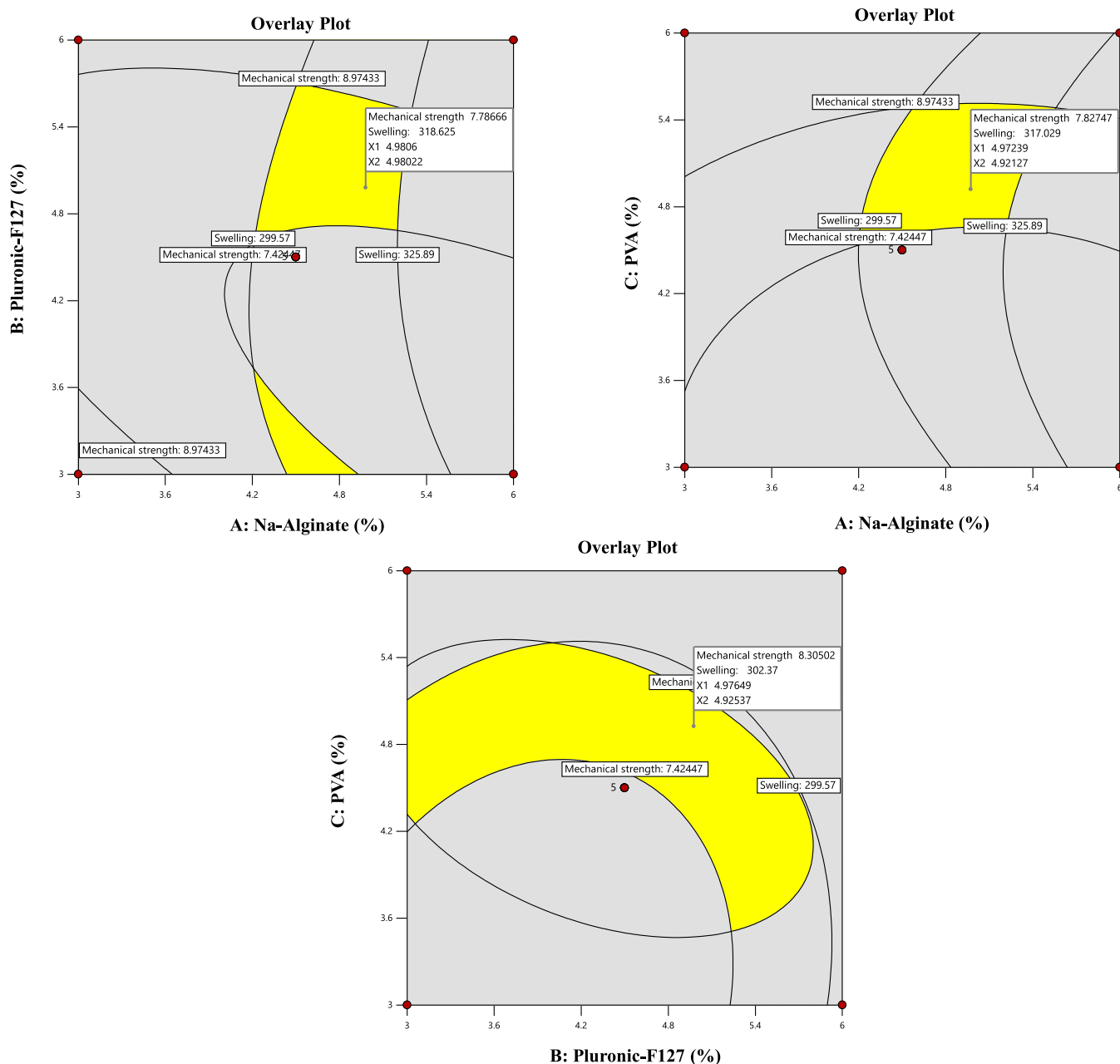
Figure 3. Overlay plots showing interactions of the optimized formulation.

drug-loaded hydrogel, and pure naringenin was studied using X-ray diffraction. The XRD pattern of naringenin at 2° angles showed dispersed sharp, thin, and strong peaks, indicating that this therapeutic agent has a crystalline structure. The polymeric materials (Na-alginate, F-127, and PVA) employed in the fabrication of the hydrogel showed an amorphous nature, as evidenced by the blank hydrogel, which displayed minor peaks at 19 and 22.5° with a halo pattern. A peak formed as the drug and polymers joined to form crystalline microaggregates after the drug was integrated into the drug-loaded hydrogel. The diffraction pattern demonstrated the compatibility of the hydrogel with the drug, and the drug release will be sustained because the hydrogel is amorphous in nature.[23]

DSC Analysis. Differential scanning calorimetry (DSC) is a well-known method used to quantify physicochemical differences in the heat capacity of crystalline medicines when they are put into hydrogels. The DSC data (Figure 6) also reveal

one endothermic and one exothermic peak at temperatures between 119 °C and over 249.32 °C. The melting temperature for Na-alginate is shown by the first peak, and polymer breakdown is responsible for the second peak. Naringenin displayed a strong peak at 254.47 °C with a heat of fusion of −149.58 J/g, showing that naringenin is crystalline. F-127 at 58.19 °C displayed one broad exothermic peak, attributed to the enthalpy of the micelles that make up its structure. The DSC graph depicts that an exothermic peak of PVA at 224.18 °C indicates thermal pyrolysis of PVA. The exothermic peaks of the drug-loaded hydrogel at 147.74 and 268.35 °C showed that the polymeric material was physically bound, and the newly created structure gives the formulation thermal stability.[24−26]

Mechanical Strength. The mechanical characteristics of wound dressings perform vital functions in the healing of wounds by acting as a barrier against infection and
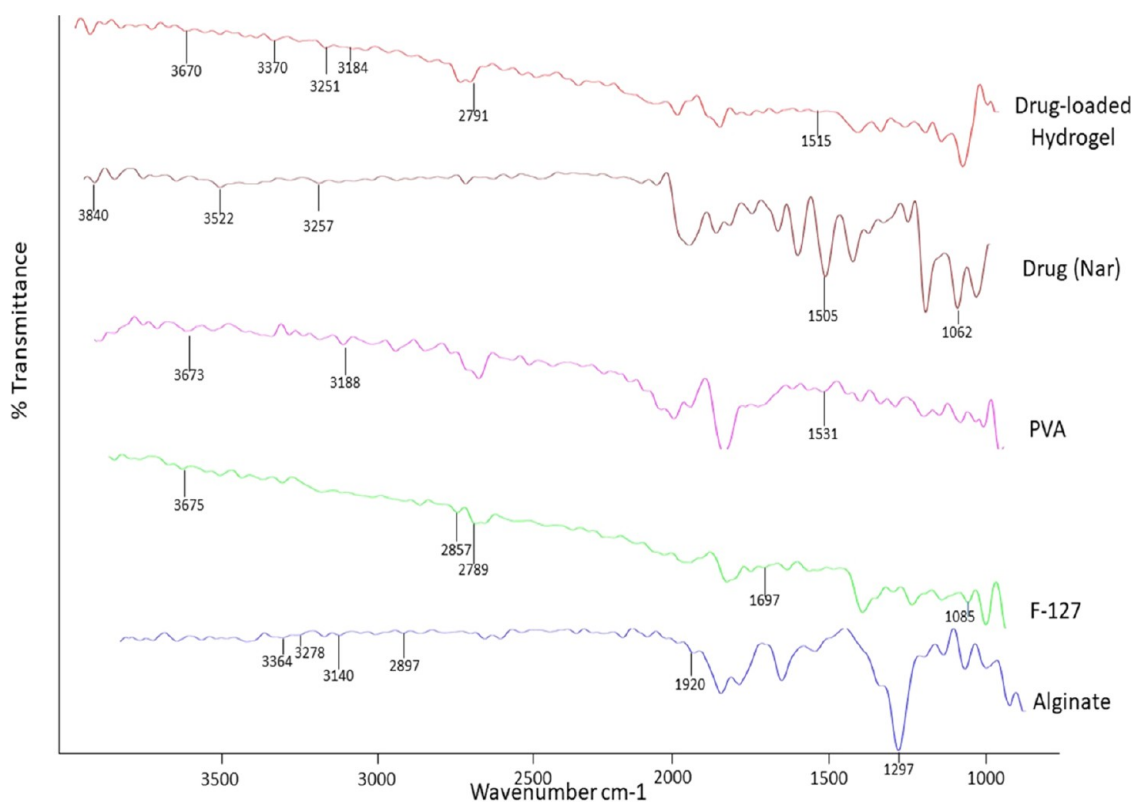
Figure 4. FTIR spectra of drug-loaded hydrogel, drug (naringenin), PVA, F-127, and Na-alginate.
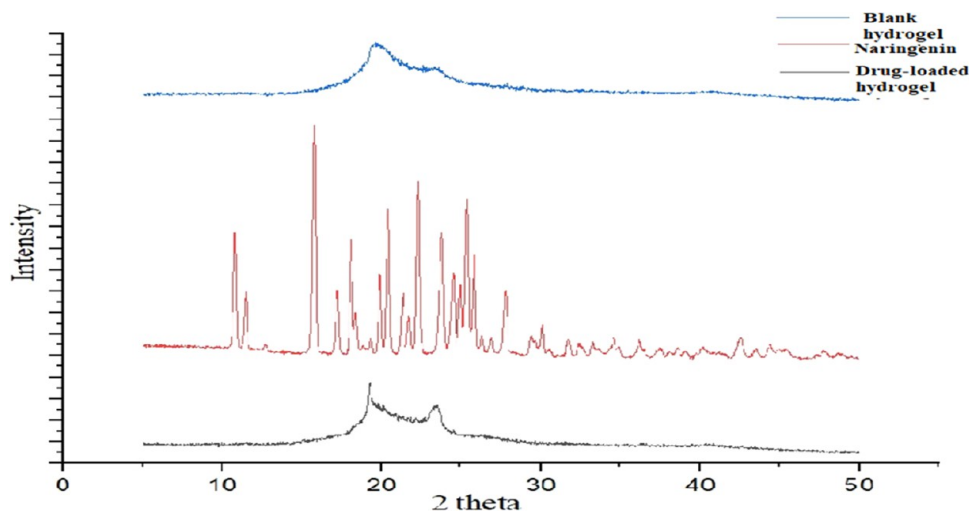

Figure 5. X-ray diffraction of blank hydrogel, naringenin (drug), and drug-loaded hydrogel.

contamination and retaining their integrity. The membrane of hydrogel would also retain and exemplify various characteristics while not causing breakage. This resulting membrane of hydrogel was meager, stretchy, having a tensile strength of approximately 8 MPa, and bendable, as evidenced by the results. Furthermore, normal skin has mechanical strength of 2.5−16 MPa, which lies in the range of the mechanical properties of the produced hydrogel membrane, enabling this newly developed membrane to be used as the treatment for chronic wounds.[23]

Electronic Microscopy. The drug-loaded hydrogel surface shape revealed by SEM images is seen in Figure 7. The surface of the optimized formulation was reasonably smooth, the matrix was homogeneous and had few pores, as seen by the evidence, and the cracks had good structural integrity. The image of SEM analysis showed the surface as sloppy, compact, and granular. Therefore, the surface morphology suggested that polymers were successfully mechanically connected. The structural system was recognized whenever the outer layer of produced hydrogels had relatively small pore gaps, which appears to be beneficial for a faster healing process by ensuring that the wound site receives the best possible oxygen supply. Such tiny pore gaps prevent germs from passing through the membrane and maintain the wound's surface moist to prevent exudates from drying up. The existence of tiny pores further
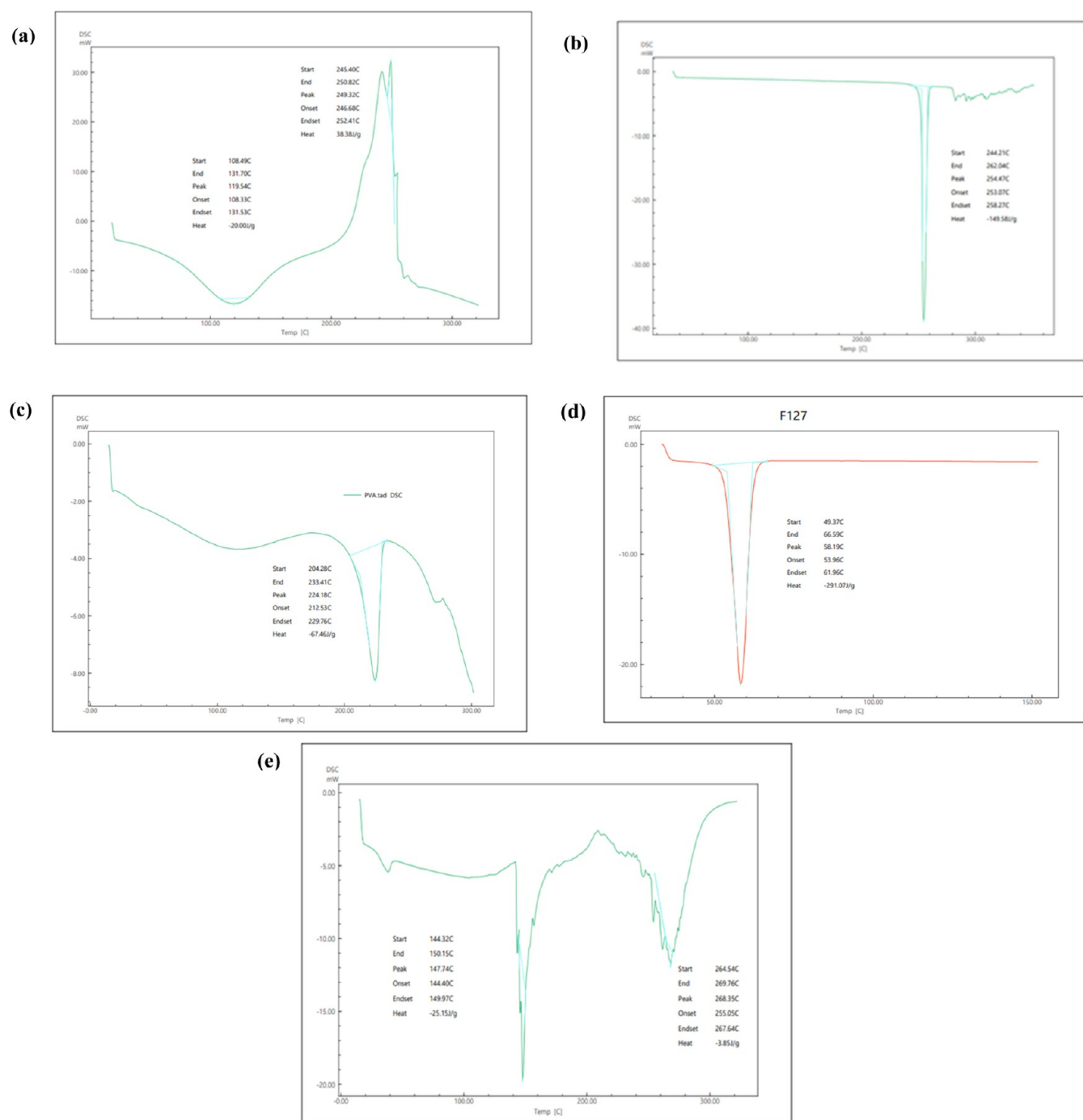
Figure 6. DSC thermogram: (a) Na-alginate, (b) naringenin, (c) PVA, (d) F-127, and (e) drug-loaded hydrogel.

suggests that these hydrogels will release drugs in a continuous manner.[25,26]

Swelling %. Swelling is a crucial characteristic that represents the polymeric materials' ability to store water and their medication release characteristics. A buffer solution with a pH of 7.4, distilled water, and normal saline was used to assess the swelling ability of hydrogels (Figure 8). The sample was found to have the best swelling in distilled water, which is indicative of the great networking of Na-alginate, PVA, and F-127. Polymer blending results in a more hydrophilic character, which aids them in retaining water. Ultimately, the extra water molecules quickly diffuse into the hydrogel network and cause it to swell. The OH groups of the PVA hydrogel swelling may

be caused by bulk hydroxyl groups that result in H-bonding with the carboxylate anion of Na-alginate in the hydrogel networks. Swelling is essential for wound healing because it affects the controlled release of therapeutic agents that are encapsulated, dressing adhesion at the wound site, and the wound exudate absorption capacity of the hydrogel from the wounded region that encourages the proliferation of fibroblasts and migration of keratinocytes.[27]

Percentage Gel Fraction. Gel fraction is an essential factor that influences the characteristics and governs the behavior of cross-linked polymers. In general, the influence of the material cross-linking reactions increases with a higher value of the gel fraction. Results of the gel fraction percentages
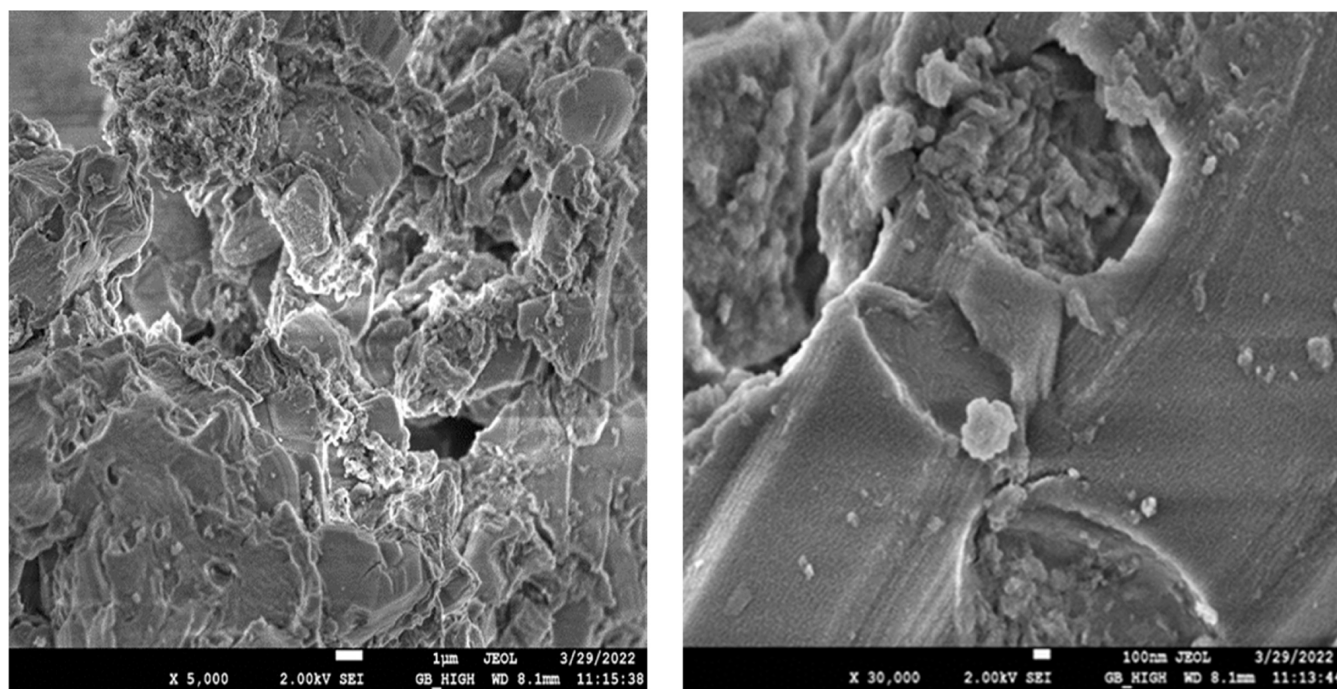
Figure 7. SEM images of the surface of drug-loaded hydrogel at different resolutions.
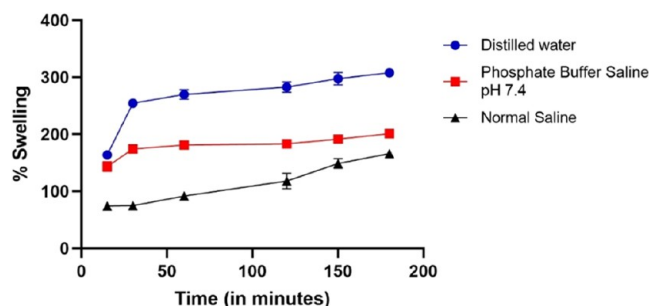

Figure 8. Swelling profile of drug-loaded hydrogel in various medias.

evaluated wound dressings in this investigation (Figure 9) had a WVTR in the mentioned range so, deemed to be good for
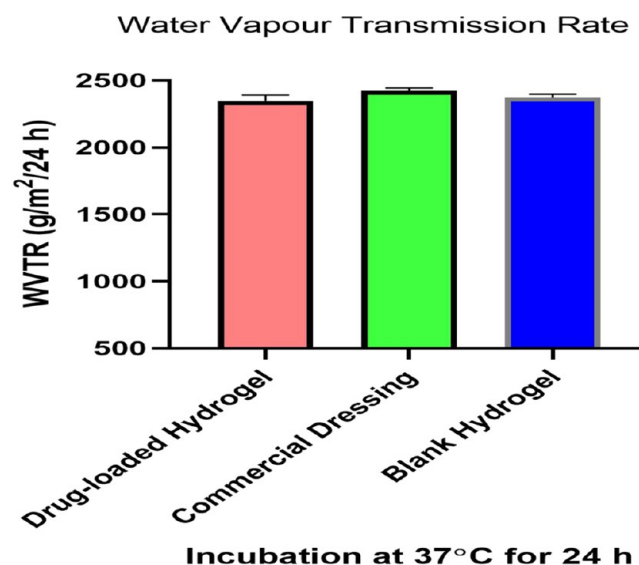

Figure 9. WVTR of different formulations.

demonstrate that as the concentration of the polymer in the preparations is elevated, the proportion of the gel fraction gets reduced. The percentage of gel fraction was 79.3% in the optimized formulation and thus, the more is its mechanical strength.[28,29]

Water Vapor Permeability. A dressing designed for the healing of wounds should ideally have an optimum water vapor transmission rate (WVTR) to deliver moist environment conditions at the wound site for proper healing of the wound, as a high WVTR level can cause dehydration in the skin and it is a lower value that causes wound exudate accumulation. The efficiency of water vapor transmission is an important element that determines the wound dressing's ability to hold water. An optimum dressing must be able to evade dryness and maintain adequate moisture and O_2 levels to ensure the best possible setting for the healing process. Normal human skin seems to have a WVTR of 204 $g/m^2/24$ h, but it was reported that injured skin has a rate of 279 $g/m^2/24$ h in the first burn injuries and 5138 $g/m^2/24$ h in granulating lesions. The optimized drug-loaded hydrogel showed a WVTR of 2361.58 $g/m^2/24$ h, and similar values of WVTR were seen in the blank hydrogel (2345.78 $g/m^2/24$ h). The WVTR of the commercial dressing was 2434.68 $g/m^2/24$ h. The optimum WVTR is estimated to be in the range of 2000−2500 $g/m^2/24$ h, and all

healing as it decreases loss of fluid and protects the body from dehydration while also limiting extensive exudate deposition, leading to an optimal wound environment.[30]

***In Vitro* Drug Release.** The therapeutic agent release from the hydrogel is displayed in Figure 10. The hydrogel exhibited faster release of therapeutic agent initially because of the higher drug concentration in the hydrogel and rapid swelling. Within the first 6 h, the burst release pattern was shown by hydrogel (45.5%) afterward, the release of residual is slowed down since there was less drug available in the hydrogel as compared to the medium. Further, increasing the amount of PVA improved the drug's release pattern. This might be because PVA has a lot
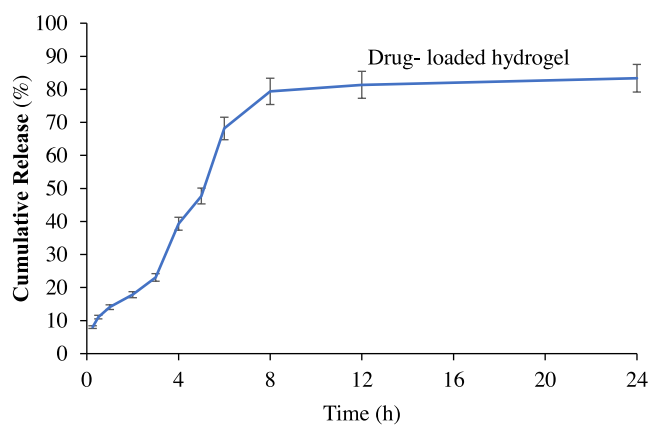
Figure 10. *In vitro* release of naringenin from hydrogel.

of hydroxyl groups, which increases its diffusion coefficient and finally drug releases. About 83.23% of the naringenin release was stabilized after 12 h suggesting the diffusion of the drug molecules across the enlarged matrix. By releasing naringenin in a regulated manner over an extended period, the prepared wound dressing in this study showed significant potential and eliminated the need for frequent dressing changes.[31−33]

Antibacterial Study. Bacterial infections cause a persistent inflammatory response at the site of infection, which prolongs the inflammatory stage of the healing process. Severe infections have the potential to slow the healing of wounds and cause sepsis. Therefore, antibacterial capability is crucial for hydrogels used to treat chronic wounds. Figure 11 depicts the negative control, there was no inhibition zone, and commercial dressing depicted 22 and 21 mm inhibition zone for *Staphylococcus aureus* and *Escherichia coli*. Through a notable suppression of bacterial growth, it was found that the drug (naringenin) plain solution showed a prominent inhibition zone against both bacterial strains that are 21 and 17.33 mm. Cross-contamination in healthcare settings, particularly in patients who are hospitalized, could quickly colonize dermal wounds with *S. aureus*. Drug-loaded hydrogels showed inhibition zones of 22 and 19 mm against *S. aureus* and *E. coli*, respectively. Gram-negative bacteria (*E. coli*) have a smaller zone because of their protective outer coat, which shields them from the environment and makes them stronger in comparison to Gram-positive bacteria.[34]

Cytocompatibility. By using the MTT assay, the impact of an incorporated drug (naringenin), drug-loaded hydrogel, blank hydrogel, commercial dressing, control group on fibroblast cell viability, and proliferation of drug-loaded hydrogel dressings was evaluated. The toxicity of dressings as well as the cell viability and proliferation of fibroblast cells on the dressing surfaces was monitored to gain insight into the cytocompatibility of dressings. Wound dressing materials should not emit any hazardous substances. The MTT assay was used to determine whether the intended dressings had any potential to release compounds with hazardous materials into the wound area. The high cell viability of all groups was ≥90 so are not hazardous (Figure 12). Furthermore, there was a slight difference in cell viability between blank and drug-loaded hydrogels. In light of this, it can be said that the produced hydrogels are nontoxic in nature and safe to use in chronic wounds.[35−37]
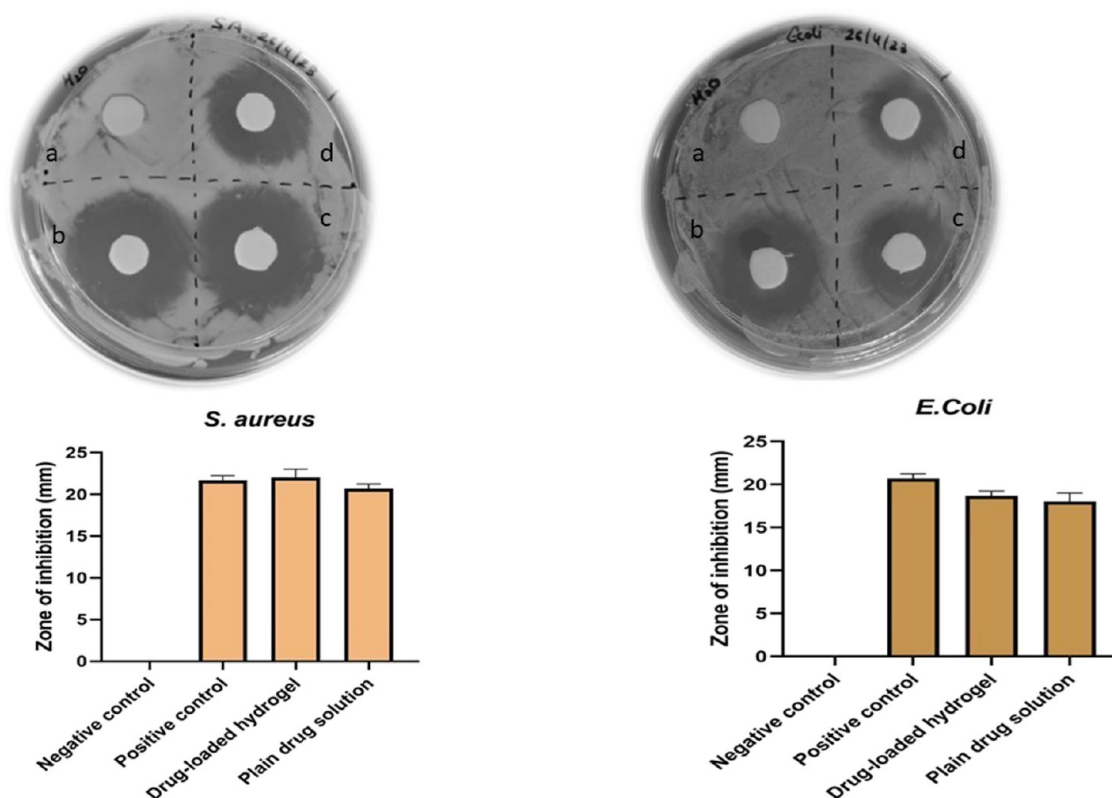

Figure 11. Antibacterial study involving *S. aureus* and *E. coli* inhibition zones on different groups: (a) negative control; (b) positive control; (c) drug-loaded hydrogel; and (d) drug plain solution.
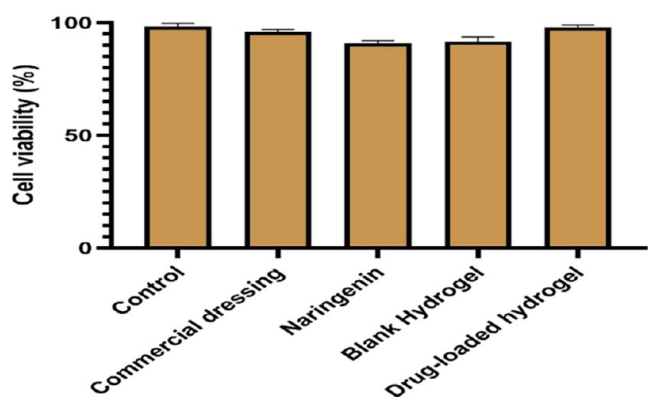
Figure 12. Cell viability % histogram for control, commercial dressing, naringenin, blank hydrogel, and drug-loaded hydrogel.

Wound Scratch Assay. An easy and affordable test called an *in vitro* scratch wound healing assay reveals important information about cell migration and proliferation over hydrogel dressings. Recovery scratches in a cell monolayer "wound gap" were evaluated at 24, 48, and 72 h (Figure 13) after scratching in order to learn more about the wound healing and wound closure capacity of the prepared dressing. Compared to the commercial dressing, migratory fibroblast cells quickly filled the scratched gap with the drug-loaded hydrogel. This occurrence is related to the drug-loaded hydrogel membrane's exceptional ability to support cellular processes correctly. After 72 h of incubation, the drug-loaded hydrogel scratched region was filled, performing significantly better than commercial dressing. The closure rate of the blank hydrogel membrane was also good, indicating the potential role of Na-alginate in wound healing. The entire closure rate of the drug-loaded hydrogel displayed fibroblast cell migration, growth, and proliferation. More convincing evidence of the drug-loaded hydrogels influence on promoting and stimulating cellular processes that aid in the healing of damaged skin tissues.[38]

***In Vivo* Study.** According to the results, the application of phytotherapeutic agents promoted wound healing by modifying inflammatory responses. Naringenin has been demonstrated to have anti-inflammatory and antioxidant properties. The hydrogel membrane loaded with naringenin demonstrated 99.9% healing and visible scars on day 21, whereas the blank hydrogel membrane group showed 93% healing of wounds. The wound treated with the drug-loaded hydrogel membrane

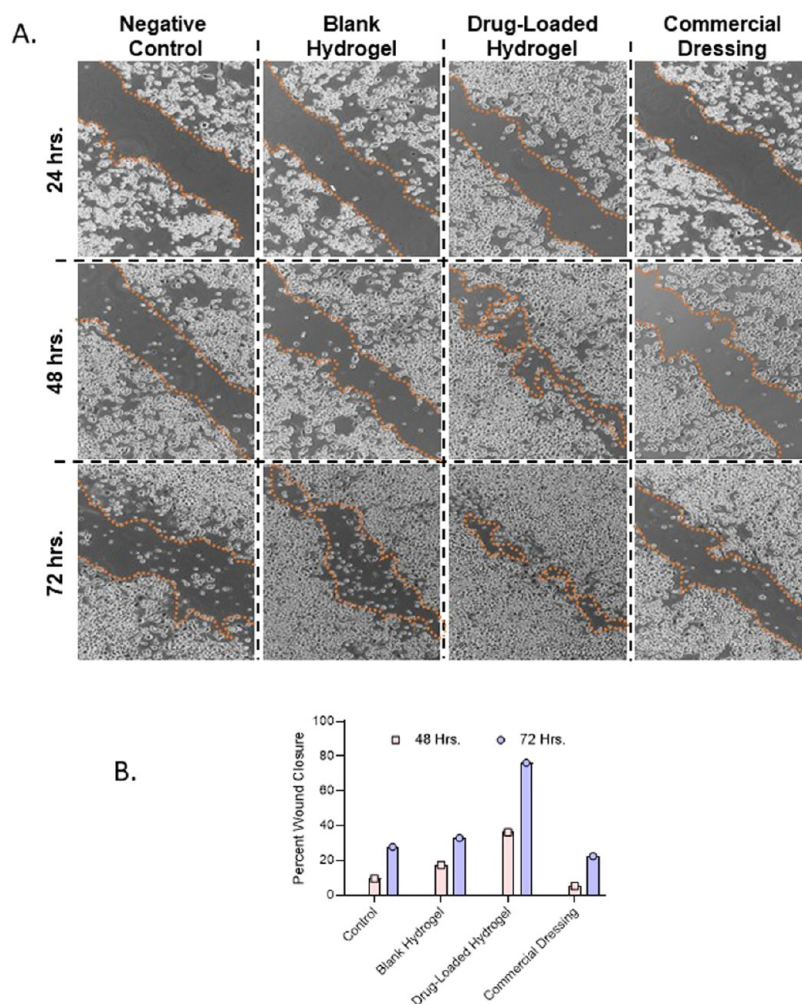**Figure 13.** (A) Photomicrographs of *in vitro* scratch assay performed in L929 murine fibroblast cells at time intervals 24, 48, and 72 h for assessment of cellular migration potential upon treatment with the blank hydrogel and drug-loaded hydrogel compared with the commercial dressing. (B) Bar plot presents the percent wound closure in each tested group at 48 and 72 h. with respect to the wound area at 24 h. in the respective groups.
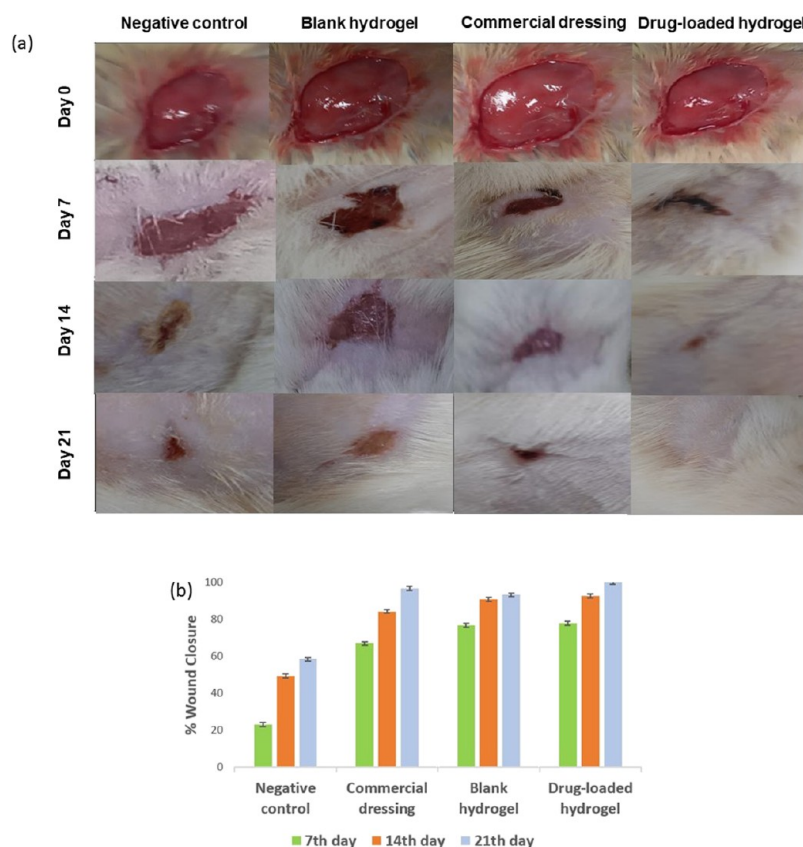
Figure 14. (a) Results of *in vivo* wound healing experiments on days 0, 7, 14, and 21. (b) Percent wound closure of different groups on 7th, 14th, and 21st day of excision.
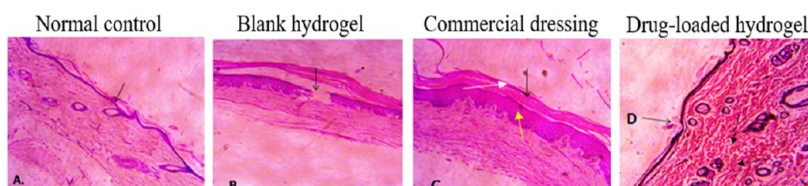

Figure 15. Representative histology images of wound sections from several groups stained with hematoxylin and eosin on the 21st day.

exhibited greater healing in comparison to the other groups (Figure 14a). The infection was averted in the commercial dressing, blank and drug-loaded hydrogels, which also slightly sped up the healing process because Na-alginate triggered macrophages to create TNF-α, which started the inflammatory signal (stage 2 in wound healing).[39,40] Additionally, phenolic substances, including naringenin, prevent growth factor cascades, such as NF-kB. Naringenin improved the antioxidant effect on the skin and minimized the lipid peroxidation, as demonstrated by Al-Roujayee in his study on thermal burn-wounded rats. Furthermore, Shan et al. showed that using naringenin, inflammation decreased the retention of CD4+ T lymphocytes and CD68+ cells (monocyte/macrophages), as well as the proinflammatory cytokine levels like TNF-α, IL-1, and IL-6. The primary outcome variable in the excision wound model was used to determine how well naringenin could treat chronic wounds. Drug-loaded hydrogel, blank, and the commercial dressing uniformly absorbed the wound exudates. Blank and drug-loaded hydrogel dressings were effortlessly removed from the surface without causing any damage to the newly produced skin in the wound area.[41,42]

In diabetic rats wound models, macroscopic photographs of full-thickness wounds were collected with the help of a digital camera at 0, 7, 14, and 21 days to assess the wound healing capacity of the drug-loaded hydrogel membranes with all other groups. The proportion of the wound size that was still exposed was estimated through a comparison of the wound size at each time point with wound size on day 1 (Figure 14a) Drug-loaded hydrogel showed expedited healing in comparison to other groups. It has been found that Na-alginate also speeds up the healing of wounds as it aids in encouraging tissue granulation and cell proliferation, which results in accelerated wound healing (Figure 14b). The drug-loaded hydrogel has a better capacity to absorb water and retain moisture, mimics ECM, and keeps the wound moist.

The results of the histological study of the specimens obtained provided additional support for the wound healing findings. Staining could be used to mark the inflammatory cells in this process and observe the deposition of fibroblasts and collagen.[43−47] The improvement in healing was examined using microscopic histological examination, which involved the quantitative analysis of a number of variables, including inflammatory cells, epithelization, and granulation tissue

formation. Figure 15 displays the H&E staining of dissected tissues from each of the treated animal groups. The recruitment of inflammatory cells to the wound site decreased by day 21 postwounding. It is reported that untreated chronic wounds get stuck in the inflammation stage of the wound healing, so the negative control group has significantly more inflammatory cells than the positive control group (commercial dressing). The drug-loaded hydrogel and commercial dressing had many fibroblasts compared to the blank hydrogel. The arrangement and distribution of collagen are important criteria for assessing wound healing. Appropriate collagen deposition favors wound repair, whereas excessive and disorganized collagen deposition causes scar hypertrophy and deters wound repair. In contrast to the immature and loose collagen identified in the negative control, mature collagen was formed in the commercial, blank, and drug-loaded hydrogels. In the case of the blank and drug-encapsulated hydrogel group, a granulating layer was seen. The development of the granulating layer is evidenced that the drug-loaded hydrogel offered antioxidant action and reduction in inflammation, thereby providing a more favorable environment for healing.[47−50]

CONCLUSIONS

Chronic wound management has received a lot of attention due to the high cost of medical expenses. In order to address the drawbacks of conventional wound dressings, efforts are being made to create and assess alternative and effective platforms for wound healing applications. Hydrogels have gained more interest as dressing materials because of their adaptable chemical, physical, and biological properties. In the current investigation, the hydrogel of Na-alginate, F-127, and PVA was created by using the solvent casting technique. A drug-loaded hydrogel effectively protected wounds against bacterial attack. The formed hydrogel is homogeneous, slightly opaque, manageable, flexible, and conformable and exhibits partial cell adhesiveness, indicating that it can protect the wound while also allowing for painless removal without causing additional damage. Due to its high capacity for swelling, the developed hydrogel absorbed the fluids of the wound bed. Additionally, naringenin, which prevented the growth of both Gram-positive and Gram-negative bacterial species, was released gradually. According to *in vivo* data, the produced hydrogel may have a suitable antibacterial impact and a sufficient therapeutic efficacy in the treatment of chronic wounds by eliminating ROS and accelerating the processes of epithelialization and collagen synthesis. The developed formulation prevented bacterial retentivity, which is crucial for wound dressing, as well as *E. coli* infiltration, supporting its protective effect against bacterial infection. This study provides a new strategy for the design of new clinical wound dressings.

EXPERIMENTAL SECTION

Materials. Naringenin and glycerol were procured from TCI Chemicals. Na-alginate (SA) (MW. 215.121 g/mol) was obtained from HiMedia Laboratories. Pluronic F-127 (MW. 9840−14,600 g/mol) and PVA (approximately 1,15,000) were obtained from Sigma-Aldrich (India). Potassium hydrogen phosphate (KH_2PO_4), formalin (37%), sodium hydroxide (NaOH), and nutrient agar were of analytical grade.

Preparation Methodology. Hydrogel membranes were fabricated by a solvent casting method with little modification. PVA (5% w/w) and Na-alginate (3% w/w) solutions were prepared in hot water separately (60−80 °C) until forming a clear solution. Pluronic F-127 was dissolved in cold water at 2−4 °C at 120 rpm, while naringenin (0.5% w/w) was dissolved at room temperature conditions in a small amount of isopropyl alcohol. Before final mixing, all formed solutions were kept under room temperature conditions. Naringenin solution was added slowly to the F-127 solution, and then, Na-alginate and PVA were added to F-127 with constant stirring. Lastly, glycerin (8% w/w) was poured into the final solution with stirring. Vigorous sonication of the final solution was carried out to eliminate entrapped air. To achieve a smooth membrane, Petri plates having a diameter of 8.5 cm were employed for casting roughly 31 g of the formed solution, plates were placed at 37 °C overnight drying in an incubator, and dry membranes were removed the next day from the Petri plates.[17]

Response Surface Optimization: Box−Behnken Design. Based on the prior literature, experiments, and brainstorming discussions among the members of the research group, various crucial factors were identified, and response optimization using a second-order three-factors-two-levels (2^3) Box−Behnken Design was carried out using Design Expert software (ver. 13, Stat-Ease. Inc.).[19] The numerous critical material attributes (CMAs) (i.e., Na-alginate, PVA, and pluronic F-127) and critical process parameters (CPPs) (i.e., drying time and temperature) were constant throughout the study on the chosen CQAs, viz., mechanical strength and swelling % of the hydrogel as per the established strategies.[20] Table 1 lists a total of 17 runs for the subsequent experimental tests employing the selected CMAs at three different levels (low (−1), medium (0), and high (+1) levels of CMAs/CPPs) in accordance with BBD. In order to determine the effects of input variables having the greatest influence on the selected CQAs, further analysis of the received data was done.

The different CQAs, like mechanical strength and swelling (%) of the fabricated hydrogel membrane, were assessed according to the standard procedures. Following that, mathematical modeling was done, and several statistical parameters were assessed to confirm which model fits the experimental data the best. The response surface methodology was used to investigate the relationships between the chosen CMAs and CQAs.

Characterization of Prepared Hydrogel Membrane. *Fourier Transform Infrared (FTIR) Spectroscopy.* A versatile method for analyzing polymers, drugs, and final formulations is FTIR. The diffuse reflectance approach was employed to analyze the functional groups present in the samples using a spectrometer (IR, affinity, DRS-8000A, Shimadzu, Japan). In order to identify the structure and functional groups, dried samples were carefully combined with a minimal quantity of dried potassium bromide before being put into a sample tube with a cup-like form. Further analysis of the infrared area between 400 and 4000 cm^{-1} was carried out.[22]

XRD Analysis. Through the use of an analytical powder diffractometer, an analysis of the drug-loaded hydrogel membrane, naringenin, and the blank membrane was carried out. The specimens were sliced for the complete enclosing of square tiles of the sample chamber, and a hydrogel membrane width of 0.5 mm was maintained. Copper Kα was employed as a source of radiation to examine these specimens over a temperature range of 10−100°, with a scanning speed of 0.02°/min.[51]

Differential Scanning Calorimetry (DSC). The differential scanning calorimetric analysis was carried out using a diffraction scanning calorimeter (PerkinElmer). In a nitrogen environment, samples were heated between 30 and 300 °C at a rate of 10 °C/min while being placed in an aluminum pan.[52−54]

Mechanical Strength. A universal testing machine (Instron-2700) was employed to study the mechanical characteristics of the hydrogel membranes. The hydrogel membrane was sliced into the required size of 1.5×3 cm^2 and subjected to 100 N/mm^2 strain.[23]

Electron Microscopy. A scanning electron microscope was used to examine the surface of the hydrogel membrane (JEOL JSM IT 300LV). The hydrogel membrane surface was analyzed by using a scanning electron microscope (JEOL JSM IT 300LV). The membrane adhered to the stub made up of aluminum with double adhesion graphite tape that was threaded with gold and had a specified width of 300. With 20 kV accelerating current, the sample solution was monitored under different resolutions.[25,26]

Swelling (%). The sample of the hydrogel membrane was sliced into the dimension of 5 cm × 5 cm and then dipped in PBS having pH 7.4 for various time intervals at 37 °C. The membranes, after immersing, were removed from the solution, and excess water was eliminated with the help of filter paper.[27] The swollen membranes were then weighed using the formula

$$W\% = \frac{m_e - m_o}{m_o} \times 100\% \tag{2}$$

where m_e is the weight of swelled hydrogels, m_o is the weight of initially dried hydrogel membranes, and $W\%$ is the percentage swelling.

Determination of Gel Fraction. The fabricated hydrogel membrane was sliced into 2×2 cm^2 and then placed in an incubator for 6 h duration for drying and weighing (W_0). The dried hydrogel was drenched for 48 h to reach an equilibrium swelling weight in distilled water, and no additional upsurge in weight could be detected. Overnight drying of samples was carried out in an incubator at 37 °C, followed by weighing again (W_e).[28,29] The equation mentioned below was used for determining % gel fraction

$$\text{gel fraction (GF\%)} = (W_e/W_0) \times 100 \tag{3}$$

Water Vapor Permeability. The technique of WVTR measurement involves the use of vials having an 18 mm diameter filled with 10 mL of distilled water. The round piece was cut from the respective formulations, and the mouth of the vials was covered. After that, Teflon tape was employed to gently airtighten these vials. Following weighing, the vials were placed in an incubator at 37 °C for a duration of 24 h. The vials were again weighed after 24 h, and the WVTR was determined[30] using eq 4

$$\text{WVTR} = \frac{(W_i - W_f)}{(A \times 24)} \times 10^6 \,(\text{gm}^2 \cdot 24\text{h}) \tag{4}$$

Drug Release. For drug release investigation, a Franz diffusion cell was employed with a cellulose acetate membrane and phosphate buffer solution having 7.4 pH maintained at 37 °C. Fresh dissolution medium was added in place of the 1 mL solution at regular intervals for 24 h. 2×2 cm^2 hydrogel membranes were added to the buffer solution and incubated at 37 °C. The concentration of released naringenin was calculated at 292 nm spectrophotometrically over the course of 24 h.[31−33]

Antibacterial Study. The antibacterial action of negative control, drug-loaded hydrogel, plain drug solution, and (blank) hydrogel was conducted on bacterial species, namely, *S. aureus* and *E. coli*. Drug-loaded hydrogels, blank hydrogel (negative control), and naringenin (10 μg/disc, positive control) were positioned onto the nutrient agar plates grown at 37 °C for 24 h. By measuring the diameters of the inhibitory zones in mm, the antibacterial action of all groups was assessed.[34]

Cytocompatibility. On L929 fibroblasts, the leachates that were recovered by soaking the hydrogel membrane in the culture media at 37 °C were evaluated for cytotoxicity. Drug-loaded hydrogels were employed for the evaluation of fibroblast cell proliferation using the procedure below. First, 1 mL of fibroblast cells (L929) was seeded at a density of 5×10^4 cells/mL into specimens with a surface area of 1 cm^2 that had been fixed on a 96-well plate. The unattached cells in the hydrogel/cell constructions were isolated after 48 h of incubation, followed by PBS washing, and the 3-(4,5-dimethylthiazol-2-yl)-2,5-diphenyltetrazolium bromide (MTT) assay was then carried out.[35]

$$\text{cell viability (\%)} = \left(\frac{\text{OD}_\text{sample} - \text{OD}_\text{positive control}}{\text{OD}_\text{negative control}} \right) \tag{5}$$

Wound Scratch Assay. Using an in vitro wound scratch experiment, the drug-loaded hydrogel (membrane) capacity to influence cellular migration and proliferation was evaluated. L929 cells were cultivated in 12-well plates at a density of 5×10^5 cells per well until they had attained 80% confluency. Then, employing a sterile 1000 L pipet tip, a cultivated cell monolayer on a drug-loaded hydrogel was scraped. By taking pictures at specific intervals, the migration of the scratched area's L929 fibroblast cells was observed.[38]

***In Vivo* Study.** *Diabetic Animal Model.* Male Wistar rats having a weight between 190 ± 10 g were chosen for the wound repair examination after receiving approval from the DPSRU Institutional Animal Ethics Committee. The polycarbonate rat cages were used for keeping animals in normal climate-controlled spaces, and they had an unrestricted entry to water and food. For inducing diabetes in Wistar rats, injection of streptozotocin via an intraperitoneal route was given with a dose of 50 mg/kg in a citrate buffer solution with a pH of 4.5 and a concentration of 0.1 M. Serum glucose testing was used to confirm diabetes, and rats who had blood sugar levels greater than or equal to 300 mg/dL for at least 3 days were chosen for the further investigation. Using a glucose meter, the serum glucose was measured daily throughout the experiments before and after STZ injection (glucometer, gluco-chek). An excisional diabetic wound model was used to study the wound healing cascade. Briefly, under xylazine and ketamine anesthesia, with the help of a biopsy punch, a 2×2 cm^2 full-thickness excisional wound was formed on the dorsal thoracic lumber of rats. The four treatment groups were randomly assigned. A total of 24 rats were categorized into four groups, each one with six rats. Group 1 included rats whose normal wounds were cleaned just with the saline solution; the group was designated as a negative control. The diabetic wounds of rats in group 2 were cleaned, and the treatment was given using a blank hydrogel. The rats in group 3 were administered commercial dressing as a positive control. Rats in group 4 were treated with a drug-loaded hydrogel as a

treatment for the wounds. At predetermined intervals after injury 0, 7, 14, and 21, digital pictures of the injured area were taken.[41−44] The wounded region was measured by using a scale, and the formula was used to determine the percentage of wound contraction.

$$\text{percentage of wound contraction}$$
$$= \frac{\text{initial wound size} - \text{specific day wound size}}{\text{initial wound size}} \times 100 \tag{6}$$

Histopathology. Granulating tissues were taken out and preserved in a 10% formalin solution. Before samples were embedded in paraffin blocks for histopathological investigation, they were dehydrated using a graded series of methanol or ethanol. A sludge microtome was used to slice the tissue into 5 m thick slices, which were then stained using Masson's trichrome and hematoxylin along with eosin (H&E) to determine how much collagen fibers and granulating tissue were visible at the wound site. Then, these results were examined at a magnification of 40 using an optical microscope (Nikon Eclipse, 50ipol).[40]

Data Analysis. The mean standard deviation (SD) is used to express the values for all measurements. The error bars represent the SD. When necessary, the t-test and one- or two-way analysis of variance (ANOVA) with post-test were employed to look at differences between the variables. The p-value of less than <0.5 was regarded as statistically significant.

ASSOCIATED CONTENT

Special Issue Paper

Published as part of the ACS Omega virtual special issue "Phytochemistry".

AUTHOR INFORMATION

Corresponding Author

   Madhu Gupta − *Department of Pharmaceutics, School of Pharmaceutical Sciences, Delhi Pharmaceutical Sciences and Research University (DPSRU), New Delhi 110017, India;* ⊙ orcid.org/0000-0002-8503-0609;
   Email: madhugupta98@gmail.com

Authors

   Neha Raina − *Department of Pharmaceutics, School of Pharmaceutical Sciences, Delhi Pharmaceutical Sciences and Research University (DPSRU), New Delhi 110017, India*

   Shafiul Haque − *Research and Scientific Studies Unit, College of Nursing and Allied Health Sciences, Jazan University, Jazan 45142, Saudi Arabia; Gilbert and Rose-Marie Chagoury School of Medicine, Lebanese American University, Beirut 11022801, Lebanon; Centre of Medical and Bio-Allied Health Sciences Research, Ajman University, Ajman 13306, United Arab Emirates;* ⊙ orcid.org/0000-0002-2989-121X

   Hardeep Singh Tuli − *Department of Bio-Sciences and Technology, Maharishi Markandeshwar Engineering College, Maharishi Markandeshwar (Deemed to Be University), Mullana-Ambala 133207, India*

   Atul Jain − *Department of Pharmaceutics, Delhi Institute of Pharmaceutical Sciences and Research, Delhi Pharmaceutical Sciences and Research University (DPSRU), New Delhi 110017, India*

   Petr Slama − *Laboratory of Animal Immunology and Biotechnology, Department of Animal Morphology, Physiology and Genetics, Faculty of AgriSciences, Mendel University in Brno, 61300 Brno, Czech Republic*

Complete contact information is available at:
https://pubs.acs.org/10.1021/acsomega.3c04441

Notes

The authors declare no competing financial interest.

ACKNOWLEDGMENTS

REFERENCES

(1) Khan, M. A. B.; Hashim, M. J.; King, J. K.; Govender, R. D.; Mustafa, H.; Al Kaabi, J. Epidemiology of type 2 diabetes—global burden of disease and forecasted trends. *J. Epidemiol. Global Health* **2020**, *10* (1), 107.

(2) Spampinato, S. F.; Caruso, G. I.; De Pasquale, R.; Sortino, M. A.; Merlo, S. The treatment of impaired wound healing in diabetes: looking among old drugs. *Pharmaceuticals* **2020**, *13* (4), 60.

(3) Patel, S.; Srivastava, S.; Singh, M. R.; Singh, D. Mechanistic insight into diabetic wounds: Pathogenesis, molecular targets and treatment strategies to pace wound healing. *Biomed. Pharmacother.* **2019**, *112*, 108615.

(4) Kujath, P.; Michelsen, A. Wounds—From physiology to wound dressing. *Dtsch. Ärzteblatt Int.* **2008**, *105* (13), 239.

(5) Brumberg, V.; Astrelina, T.; Malivanova, T.; Samoilov, A. Modern wound dressings: hydrogel dressings. *Biomedicines* **2021**, *9* (9), 1235.

(6) Wu, L.; He, Y.; Mao, H.; Gu, Z. Bioactive hydrogels based on polysaccharides and peptides for soft tissue wound management. *J. Mater. Chem. B* **2022**, *10*, 7148−7160.

(7) Raina, N.; Pahwa, R.; Thakur, V. K.; Gupta, M. Polysaccharide-based hydrogels: New insights and futuristic prospects in wound healing. *Int. J. Biol. Macromol.* **2022**, *223*, 1586−1603.

(8) Beaumont, M.; Tran, R.; Vera, G.; Niedrist, D.; Rousset, A.; Pierre, R.; Shastri, V. P.; Forget, A. Hydrogel-forming algae polysaccharides: from seaweed to biomedical applications. *Biomacromolecules* **2021**, *22* (3), 1027−1052.

(9) Aderibigbe, B. A.; Buyana, B. Alginate in wound dressings. *Pharmaceutics* **2018**, *10* (2), 42.

(10) Shah, S. A.; Sohail, M.; Khan, S.; Minhas, M. U.; De Matas, M.; Sikstone, V.; Hussain, Z.; Abbasi, M.; Kousar, M. Biopolymer-based biomaterials for accelerated diabetic wound healing: A critical review. *Int. J. Biol. Macromol.* **2019**, *139*, 975−993.

(11) Lee, K. Y.; Mooney, D. J. Alginate: properties and biomedical applications. *Prog. Polym. Sci.* **2012**, *37* (1), 106−126.

(12) Kamoun, E. A.; Kenawy, E. R.; Chen, X. A review on polymeric hydrogel membranes for wound dressing applications: PVA-based hydrogel dressings. *J. Adv. Res.* **2017**, *8* (3), 217−233.

(13) Kant, V.; Gopal, A.; Kumar, D.; Gopalkrishnan, A.; Pathak, N. N.; Kurade, N. P.; Tandan, S. K.; Kumar, D. Topical pluronic F-127 gel application enhances cutaneous wound healing in rats. *Acta Histochem.* **2014**, *116* (1), 5−13.

(14) Raina, N.; Rani, R.; Pahwa, R.; Gupta, M. Biopolymers and treatment strategies for wound healing: an insight view. *Int. J. Polym. Mater. Polym. Biomater.* **2022**, *71* (5), 359−375.

(15) Salehi, B.; Fokou, P. V.; Sharifi-Rad, M.; Zucca, P.; Pezzani, R.; Martins, N.; Sharifi-Rad, J. The therapeutic potential of naringenin: a review of clinical trials. *Pharmaceuticals* **2019**, *12* (1), 11.

(16) Rauf, A.; Shariati, M. A.; Imran, M.; Bashir, K.; Khan, S. A.; Mitra, S.; Emran, T. B.; Badalova, K.; Uddin, M. S.; Mubarak, M. S.; Aljohani, A. S.; et al. Comprehensive review on naringenin and naringin polyphenols as a potent anticancer agent. *Environ. Sci. Pollut. Res.* **2022**, *29* (21), 31025−31041.

(17) Yu, L. X.; Amidon, G.; Khan, M. A.; Hoag, S. W.; Polli, J.; Raju, G. K.; Woodcock, J. Understanding pharmaceutical quality by design. *AAPS J.* **2014**, *16*, 771−783.

(18) Alavi, T.; Rezvanian, M.; Ahmad, N.; Mohamad, N.; Ng, S. F. Pluronic-F127 composite film loaded with erythromycin for wound application: formulation, physicomechanical and in vitro evaluations. *Drug Delivery Transl. Res.* **2019**, *9*, 508−519.

(19) Singh, B.; Dahiya, M.; Saharan, V.; Ahuja, N. Optimizing drug delivery systems using systematic″ design of experiments.″ Part II: retrospect and prospects. *Crit. Rev. Ther. Drug Carrier Syst.* **2005**, *22* (3), 215−294.

(20) Sharma, R.; Pahwa, R.; Ahuja, M. Iodine-loaded poly (silicic acid) gellan nanocomposite mucoadhesive film for antibacterial application. *J. Appl. Polym. Sci.* **2021**, *138* (2), 49679.

(21) Shafique, M.; Sohail, M.; Minhas, M. U.; Khaliq, T.; Kousar, M.; Khan, S.; Hussain, Z.; Mahmood, A.; Abbasi, M.; Aziz, H. C.; Shah, S. A. Bio-functional hydrogel membranes loaded with chitosan nanoparticles for accelerated wound healing. *Int. J. Biol. Macromol.* **2021**, *170*, 207−221.

(22) Abbasi, A. R.; Sohail, M.; Minhas, M. U.; Khaliq, T.; Kousar, M.; Khan, S.; Hussain, Z.; Munir, A. Bioinspired Na-alginate based thermosensitive hydrogel membranes for accelerated wound healing. *Int. J. Biol. Macromol.* **2020**, *155*, 751−765.

(23) Pereira, R.; Carvalho, A.; Vaz, D. C.; Gil, M. H.; Mendes, A.; Bártolo, P. Development of novel alginate based hydrogel films for wound healing applications. *Int. J. Biol. Macromol.* **2013**, *52*, 221−230.

(24) Patel, S.; Srivastava, S.; Singh, M. R.; Singh, D. Preparation and optimization of chitosan-gelatin films for sustained delivery of lupeol for wound healing. *Int. J. Biol. Macromol.* **2018**, *107*, 1888−1897.

(25) Natarajan, N.; Shashirekha, V.; Noorjahan, S. E.; Rameshkumar, M.; Rose, C.; Sastry, T. P. Fibrin−chitosan−gelatin composite film: preparation and characterization. *J. Macromol. Sci. A* **2005**, *42* (7), 945−953.

(26) Postolović, K.; Ljujić, B.; Kovačević, M. M.; Đorđević, S.; Nikolić, S.; Živanović, S.; Stanić, Z. Optimization, characterization, and evaluation of carrageenan/alginate/poloxamer/curcumin hydrogel film as a functional wound dressing material. *Mater. Today Commun.* **2022**, *31*, 103528.

(27) Khan, S.; Minhas, M. U.; Ahmad, M.; Sohail, M. Self-assembled supramolecular thermoreversible β-cyclodextrin/ethylene glycol injectable hydrogels with difunctional Pluronic 127 as controlled delivery depot of curcumin. Development, characterization and in vitro evaluation. *J. Biomater. Sci., Polym. Ed.* **2018**, *29* (1), 1−34.

(28) Champeau, M.; Póvoa, V.; Militão, L.; Cabrini, F. M.; Picheth, G. F.; Meneau, F.; Jara, C. P.; de Araujo, E. P.; de Oliveira, M. G. Supramolecular poly (acrylic acid)/F127 hydrogel with hydration-controlled nitric oxide release for enhancing wound healing. *Acta Biomater.* **2018**, *74*, 312−325.

(29) Hwang, M. R.; Kim, J. O.; Lee, J. H.; Kim, Y. I.; Kim, J. H.; Chang, S. W.; Jin, S. G.; Kim, J. A.; Lyoo, W. S.; Han, S. S.; Ku, S. K.; et al. Gentamicin-loaded wound dressing with polyvinyl alcohol/dextran hydrogel: gel characterization and in vivo healing evaluation. *AAPS PharmSciTech* **2010**, *11*, 1092−1113.

(30) Xu, R.; Xia, H.; He, W.; Li, Z.; Zhao, J.; Liu, B.; Wu, J.; et al. Controlled water vapor transmission rate promotes wound-healing via wound re-epithelialization and contraction enhancement. *Sci. Rep.* **2016**, *6* (1), No. 24596, DOI: 10.1038/srep24596.

(31) Ahmed, A.; Niazi, M. B.; Jahan, Z.; Ahmad, T.; Hussain, A.; Pervaiz, E.; Janjua, H. A.; Hussain, Z. In-vitro and in-vivo study of superabsorbent PVA/Starch/g-C3N4/Ag@ TiO2 NPs hydrogel membranes for wound dressing. *Eur. Polym. J.* **2020**, *130*, 109650.

(32) Huang, Y.; Dan, N.; Dan, W.; Zhao, W. Reinforcement of polycaprolactone/chitosan with nanoclay and controlled release of curcumin for wound dressing. *ACS Omega* **2019**, *4* (27), 22292−22301.

(33) Li, X.; Nan, K.; Li, L.; Zhang, Z.; Chen, H. In vivo evaluation of curcumin nanoformulation loaded methoxy poly(ethylene glycol)-graft-chitosan composite film for wound healing application. *Carbohydr. Polym.* **2012**, *88*, 84−90.

(34) Rezvanian, M.; Amin, M. C. I. M.; Ng, S. F. Development and physicochemical characterization of alginate composite film loaded with simvastatin as a potential wound dressing. *Carbohydr. Polym.* **2016**, *137*, 295−304.

(35) Tang, X.; Gu, X.; Wang, Y.; Chen, X.; Ling, J.; Yang, Y. Stable antibacterial polysaccharide-based hydrogels as tissue adhesives for wound healing. *RSC Adv.* **2020**, *10* (29), 17280−17287.

(36) Tamahkar, E.; Özkahraman, B.; Süloğlu, A. K.; İdil, N.; Perçin, I. A novel multilayer hydrogel wound dressing for antibiotic release. *J. Drug Delivery Sci. Technol.* **2020**, *58*, 101536.

(37) Hago, E. E.; Li, X. Interpenetrating polymer network hydrogels based on gelatin and PVA by biocompatible approaches: synthesis and characterization. *Adv. Mater. Sci. Eng.* **2013**, *2013*, 1.

(38) Gharibi, R.; Shaker, A.; Rezapour-Lactoee, A.; Agarwal, S. Antibacterial and biocompatible hydrogel dressing based on gelatin- and castor-oil-derived biocidal agent. *ACS Biomater. Sci. Eng.* **2021**, *7* (8), 3633−3647.

(39) Rezapour-Lactoee, A.; Yeganeh, H.; Gharibi, R.; Milan, P. B. Enhanced healing of a full-thickness wound by a thermoresponsive dressing utilized for simultaneous transfer and protection of adipose-derived mesenchymal stem cells sheet. *J. Mater. Sci. Mater. Med.* **2020**, *31*, 101.

(40) Rezvanian, M.; Ng, S. F.; Alavi, T.; Ahmad, W. In-vivo evaluation of Alginate-Pectin hydrogel film loaded with Simvastatin for diabetic wound healing in Streptozotocin-induced diabetic rats. *Int. J. Biol. Macromol.* **2021**, *171*, 308−319.

(41) Al-Roujayee, A. S. Naringenin improves the healing process of thermally-induced skin damage in rats. *J. Int. Med. Res.* **2017**, *45* (2), 570−582.

(42) Shan, S.; Zhang, Y.; Wu, M.; Yi, B.; Wang, J.; Li, Q. Naringenin attenuates fibroblast activation and inflammatory response in a mechanical stretch-induced hypertrophic scar mouse model. *Mol. Med. Rep.* **2017**, *16* (4), 4643−4649.

(43) Thomas, A.; Harding, K.; Moore, K. Alginates from wound dressings activate human macrophages to secrete tumour necrosis factor-α. *Biomaterials* **2000**, *21*, 1797−1802, DOI: 10.1016/S0142-9612(00)00072-7.

(44) Abbas, M. M.; Al-Rawi, N.; Abbas, M. A.; Al-Khateeb, I. Naringenin potentiated β-sitosterol healing effect on the scratch wound assay. *Res. Pharm. Sci.* **2019**, *14* (6), 566.

(45) Zhang, Y.; Li, M.; Wang, Y.; Han, F.; Shen, K.; Luo, L.; Li, Y.; Jia, Y.; Zhang, J.; Cai, W.; Wang, K.; et al. Exosome/metformin-loaded self-healing conductive hydrogel rescues microvascular dysfunction and promotes chronic diabetic wound healing by inhibiting mitochondrial fission. *Bioact. Mater.* **2023**, *26*, 323−336.

(46) Wang, C.; Liang, Y.; Huang, Y.; Li, M.; Guo, B. Porous photothermal antibacterial antioxidant dual−crosslinked cryogel based on hyaluronic acid/polydopamine for non-compressible hemostasis and infectious wound repair. *J. Mater. Sci. Technol.* **2022**, *121*, 207−219.

(47) Wang, K.; Dong, R.; Tang, J.; Li, H.; Dang, J.; Zhang, Z.; Yu, Z.; Guo, B.; Yi, C. Exosomes laden self-healing injectable hydrogel enhances diabetic wound healing via regulating macrophage polarization to accelerate angiogenesis. *Chem. Eng. J.* **2022**, *430*, 132664.

(48) Li, D.; Chen, K.; Tang, H.; Hu, S.; Xin, L.; Jing, X.; He, Q.; Wang, S.; Song, J.; Mei, L.; Cannon, R. D.; et al. A Logic-Based Diagnostic and Therapeutic Hydrogel with Multistimuli Responsiveness to Orchestrate Diabetic Bone Regeneration. *Adv. Mater.* **2022**, *34* (11), 2108430.

(49) Cao, H.; Zhu, J.; Zhang, J.; Yang, L.; Guo, X.; Tian, R.; Wu, H.; Li, Y.; Gu, Z. In Situ Fabrication of Robust Polyphenolic Hydrogels for Skin Protection and Repair. *Chem. Mater.* **2023**, *35* (5), 2191−2201.

(50) Liu, B.; Kong, Y.; Alimi, O. A.; Kuss, M. A.; Tu, H.; Hu, W.; Rafay, A.; Vikas, K.; Shi, W.; Lerner, M.; Berry, W. L.; et al. Multifunctional Microgel-Based Cream Hydrogels for Postoperative Abdominal Adhesion Prevention. *ACS Nano* **2023**, *17* (4), 3847−3864.

(51) Wen, J.; Liu, B.; Yuan, E.; Ma, Y.; Zhu, Y. Preparation and physicochemical properties of the complex of naringenin with hydroxypropyl-β-cyclodextrin. *Molecules* **2010**, *15* (6), 4401−4407.

(52) Zhao, L.; Mitomo, H.; Zhai, M.; Yoshii, F.; Nagasawa, N.; Kume, T. Synthesis of antibacterial PVA/CM-chitosan blend hydrogels with electron beam irradiation. *Carbohydr. Polym.* **2003**, *53* (4), 439−446.

(53) Shahzad, A.; Khan, A.; Afzal, Z.; Umer, M. F.; Khan, J.; Khan, G. M. Formulation development and characterization of cefazolin nanoparticles-loaded cross-linked films of sodium alginate and pectin as wound dressings. *Int. J. Biol. Macromol.* **2019**, *124*, 255−269.

(54) Karolewicz, B.; Gajda, M.; Pluta, J.; Górniak, A. Dissolution study and thermal analysis of fenofibrate−Pluronic F127 solid dispersions. *J. Therm. Anal. Calorim.* **2016**, *125*, 751−757.